



HORIZON 2020

HORIZON 2020 RESEARCH AND INNOVATION FRAMEWORK PROGRAMME OF THE EUROPEAN ATOMIC ENERGY COMMUNITY

Nuclear Fission and Radiation Protection 2018 (NFRP-2018-4)

Project acronym: **SANDA**

Project full title: **Solving Challenges in Nuclear Data for the Safety of
European Nuclear facilities**

Grant Agreement no.: **H2020 Grant Agreement number: 847552**

Workpackage N°: **WP2**

Identification N°: **D2.5**

Type of document: **Deliverable**

Title: Report on the measurements of the branching ratio for ^{209}Bi , $^{208}\text{Pb}(n,\text{tot})$
and $^{238}\text{U}(n,\text{inel})$ cross sections at GELINA

Dissemination Level: **PU**

Reference:

Status: **VERSION 1**

Comments:

	Name	Partner	Date	Signature
Prepared by:	C. Paradela	13	04-04-2024	
WP leader:	D. Cano-Ott	1		
IP Co-ordinator:	E. González	1		

Report on the measurements of the branching ratio for ^{209}Bi , $^{208}\text{Pb}(n,\text{tot})$ and $^{238}\text{U}(n,\text{inel})$ cross sections at GELINA

Table of content

1. Introduction	3
2. Measurements for ^{209}Bi	3
2.1. $^{209}\text{Bi}(n,\gamma)$ branching ratio measurement	4
2.2. Transmission measurements.....	5
2.3. Capture measurements	7
3. Transmission on natural lead and ^{206}Pb	7
3.1. Experimental description	8
3.2. Data reduction and results	8
4. $^{238}\text{U}(n,\text{inel})$ cross sections measurements at GELINA	9
4.1. The prompt γ -ray spectroscopy method for (n, n') studies.....	9
4.2. Experimental conditions.....	9
4.3. Results	11
4.3.1. Extraction of γ -ray production cross sections.....	11
4.3.2. $(n, n' \gamma)$ cross sections.....	13
4.3.3. Branching ratios	15
4.4. Dissemination	16
5. Conclusions	16

1. Introduction

Under the framework of **Task 2.3** (Neutron elastic and inelastic scattering and neutron multiplication cross sections) in SANDA project, high accuracy measurements for the branching ratio of ^{209}Bi , $^{208}\text{Pb}(n,\text{tot})$ and $^{238}\text{U}(n,\text{inel})$ cross sections has to be performed at GELINA (Geel Electron LINear Accelerator) neutron facility operated by EC-JRC-Geel (Belgium) in response to specific requests based on the output of sensitivity studies of k_{eff} performed in CHANDA. This report, provided as the corresponding deliverable D2.5, consists of three sections, each one describing the current situation of the three different measurements proposed in the Task.

2. Measurements for ^{209}Bi

Pablo Romojaro¹, Carlos Paradela², Gery Alaerts², Luca Fiorito¹, J. Heyse², S. Kopecky², S. Moscati², P. Schillebeeckx², Alexey Santovskiy¹, Gert Van Den Eynde¹, Danny Vendelbo², Ruud Wynants², Atushi Kimura³, Shinsuke Endo³

¹Belgium Nuclear Research Center (SCK CEN), Brussels, Belgium

² European Commission, Joint Research Centre, Geel, Belgium

³Japanese Atomic Energy Agency Japan

Within CHANDA project a sensitivity study was carried out to identify reactions and nuclides of importance for the design and safety assessment of MYRRHA [1]. The cross sections for neutron interactions with Bi as target nucleus recommended in the main nuclear data libraries were compared and validated against microscopic cross section and integral experiment data [2]. These studies indicated a shortage on experimental data to produce accurate cross section and determine the energy dependence of the (n,γ) reaction to the ground and to the isomeric state of ^{210}Bi . Ground state quickly decays to strong alpha-emitter ^{210}Po that determines radiological hazard of MYRRHA lead-bismuth eutectic coolant while long-lived $^{210\text{m}}\text{Bi}$, being alpha-emitter as well, will pose long-term concern. The lack of accurate cross section data results in a poor content estimation [3], and for that reason the corresponding entry was introduced in the High Priority Request List maintained by the NEA/OECD [4].

In order to overcome the lack of experimental data, measurements were carried to obtain reliable nuclear data for bismuth. The ^{209}Bi capture measurements for determining branching ratios were carried out at J-PARC facility in Japan, where a suitable experimental setup was already available for such kind of measurements. In addition, high-resolution transmission and capture measurements based on total energy technique were performed at GELINA. A visit from S. Endo (JAEA) to JRC and SCK CEN was planned in March 2020 to assist in the analysis of the capture data taken at J-PARC. Unfortunately, due to the COVID-19 crisis it was postponed till 2023 and the analysis of J-PARC data was delayed. In the meantime, neutron transmission measurements with two metallic samples of different thicknesses (4 mm and 1.26 mm) were carried out at GELINA in 2020 and 2021. The data reduction to derive transmission from the data using the AGS code was accomplished by SCK staff assisted by JRC researchers within the project *Bismuth_MYHRA* (RIAA N° 35543/ 1 /2019-1-RD-EUFRAT-GELINA).

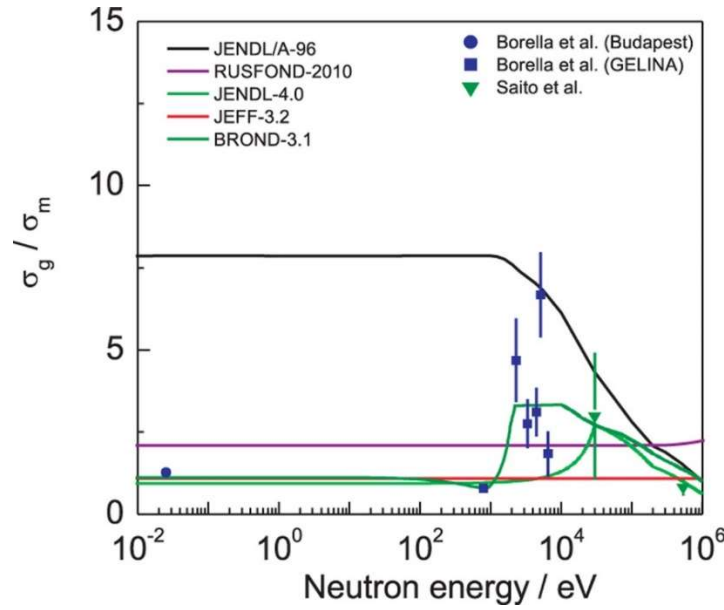


Figure 1. Comparison on ^{209}Bi branching ratio experimental data and evaluations published in ref [3].

2.1. $^{209}\text{Bi}(n,\gamma)$ branching ratio measurement

The experiment was performed at J-PARC MLF facility, a spallation neutron source where a synchrotron produces 3 GeV protons in a double-bunch mode with 25 Hz repetition rate. A detection setup based on germanium detectors is mounted at ANNRI, a beam line of MLF, at a distance of 21.5 m from the moderator. The array of germanium detectors is composed of eight coaxial-type detectors and two cluster-type detector [5]. In the capture cross section measurements, the two cluster detectors are used. The acquisition system is based on CAEN V1724 modules with 14-bit pulse height resolution and 100 MHz sampling rate, which registered the time-of-flight (TOF) and the pulse height of each detector signal. In addition of the Bi sample, Au sample was used for normalization purpose and a boron sample was used for neutron flux determination, based on the detection of the single energy gamma-ray at 477.6 keV. A carbon sample was used to determine the background produced by scattered neutrons captured by the materials around the germanium detectors. A measurement without sample was also carried out to account for the sample independent background.

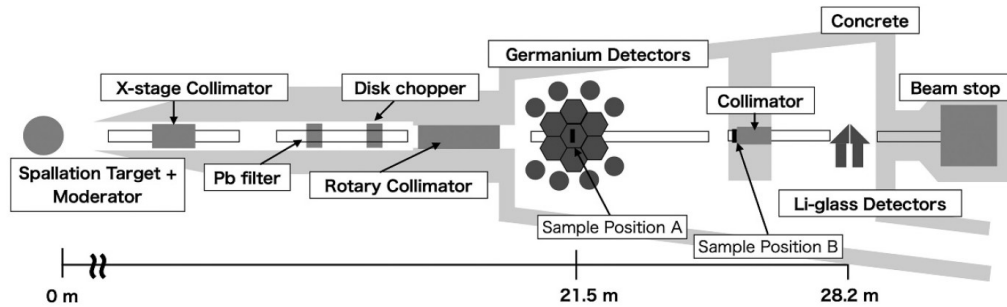


Figure 2. Top view of the ANNRI beam line obtained from reference [5].

JAEA researchers provided the raw data of the experiment together with ROOT analysis software for the data reduction and for the energy calibration of the germanium detectors using gamma sources.

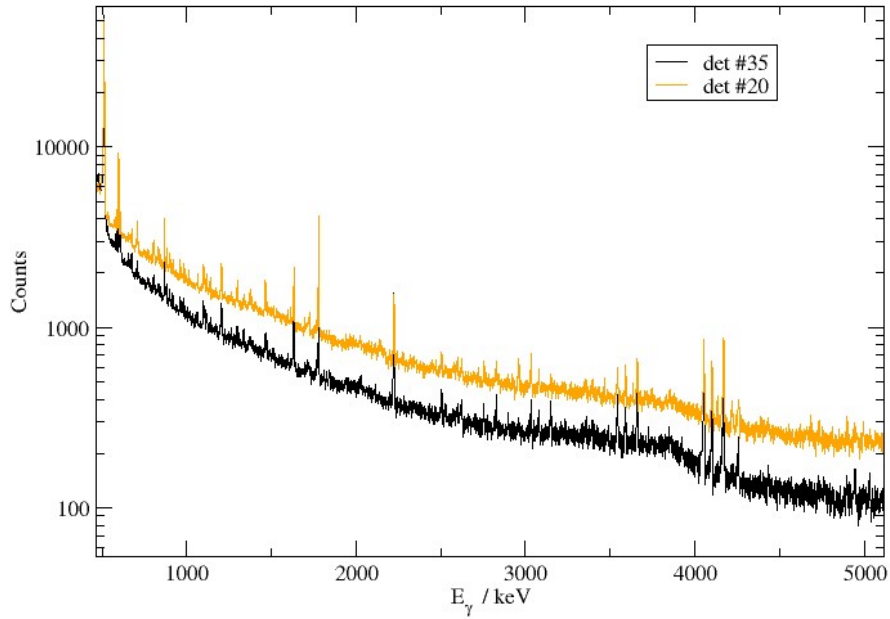


Figure 3. Energy-calibrated γ -ray spectra obtained with the bismuth sample (run 55) for the detectors labelled as 20 and 35 in the ANNRI setup.

2.2. Transmission measurements

Transmission measurements through metallic bismuth samples have been performed at the time-of-flight facility GELINA. The measurements have been carried out at a 50 m transmission station using a Li-glass scintillator with the accelerator operating at 400 Hz. An annular collimation system based on lead, nickel copper, lithium and B_4C materials was designed to define a neutron beam diameter of 45 mm at the sample position. In addition, a ^{10}B overlap filter with an areal density of about 0.08 at/b was placed close to the neutron target to minimize the contribution of slow neutrons coming from previous accelerator bursts. The impact of γ -rays in the neutron detector was reduced by a 16 mm thick lead filter.

Metallic bismuth samples of 1.25 and 4 mm nominal thickness were placed in automatic sample changers at a distance of approximately 24 m from the neutron source. This allows to take data alternating sample-in and sample-out measurements in cycles of about 600 seconds, which reduces the uncertainty on the normalization of the beam intensity. In addition, the same position has available sodium, cobalt and tungsten black resonance filters to determine the background contribution at different neutron energies providing its time dependence.

In order to detect the neutrons passing through the sample, a 151.6 mm diameter Li-glass scintillator was placed at about 47 m from the neutron target, where the neutron beam diameter was about 90 mm.

The experimental transmission T_{exp} as a function of TOF was obtained from the ratio of a sample-in measurement C_{in} and a sample-out measurement C_{out} , both corrected for their background contributions B_{in} and B_{out} , respectively:

$$T_{\text{exp}} = N \frac{C_{\text{in}} - KB_{\text{in}}}{C_{\text{out}} - KB_{\text{out}}}. \quad (3.1)$$

The factor N accounts for uncertainties due to variations in the beam intensity and K for systematic effects due to the background model. The TOF spectra, C_{in} and C_{out} , were corrected for losses due to the dead time in the detector and electronics chain. The AGS code [6] was used to derive the experimental transmission and to propagate both the correlated and uncorrelated uncertainties. The experimental transmissions obtained in this project were used to verify recommended resonance parameters for neutron interactions with ^{209}Bi . As an example of the results, Figure 3 shows the transmission through a 1.255 mm thick Bi sample in the region of the strong s-wave resonance at 800 eV. It compares the experimental transmission with the theoretical transmission derived from the resonance parameters in JENDL-4.0 and ENDF/B-VIII.0. For a better representation of the data the neutron energies were adjusted. The calculated transmission obtained with the neutron width in ENDF/B-VIII.0, which is derived from the transmission data in Ref. [7], is in much better agreement with the experimental data than the transmission calculated with the one in JENDL-4.0. The latter is adopted from Ref. [8], which is based on the capture data obtained at the n_TOF facility. This shows the shortcomings of deriving neutron widths only from capture yields for a nucleus like ^{209}Bi . For ^{209}Bi , the radiation width is in general much smaller compared to the neutron width such that the neutron width is derived from the resonance profile. This requires an accurate description of the TOF-response function.

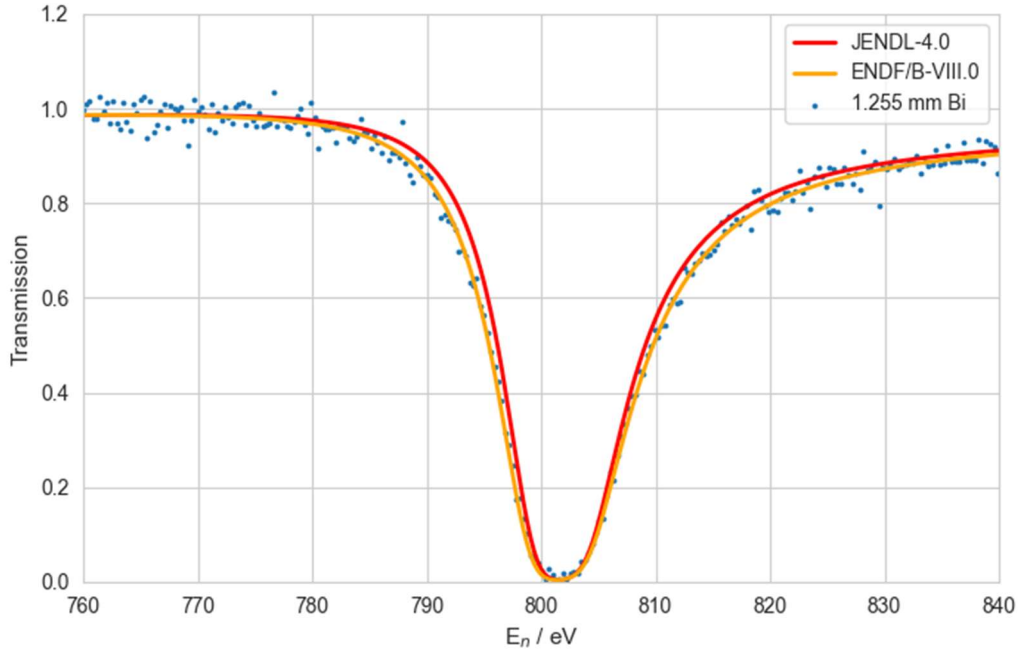


Figure 4. Comparison of the experimental and calculated transmission through the 1.255 mm thick Bi sample. The calculated transmissions are obtained with REFIT using the resonance parameters in JENDL-4.0 and ENDF/B-VIII.0, including a neutron energy adjustment to match the experimental result.

The results of the transmission measurements have been published as a JRC technical report [9] and the data submitted to EXFOR database.

2.3. Capture measurements

Capture measurements through a metallic bismuth sample of 4 mm thickness have been performed at the time-of-flight facility GELINA. The measurements have been carried out at a 60 m station of flight path 14. The moderated neutron beam is collimated to about 80 mm diameter at the sample position.

The γ -rays produced after neutron capture reactions were detected by four C_6D_6 detectors placed in the vertical and horizontal axes with respect to the sample. The detectors are positioned at an angle of 125° with respect to the direction of the neutron beam. This geometry minimizes systematic effects due to the anisotropy in the primary dipole γ -ray emission which can depend on the spin and orbital momentum of the resonances.

The energy dependence of the neutron fluence rate was measured using a Frisch-gridded ionization chamber based on the $^{10}B(n,\alpha)$ neutron cross section standard. The ionization chamber was placed at about 50 cm distance before the sample. The processing of the time and amplitude signals for both capture and fluence rate detection systems was based on analogue electronics. The TOF and the pulse height of each detected event were recorded in list mode using a data acquisition system developed at the JRC Geel [10].

In addition of the bismuth sample, measurements with a carbon sample and the empty frame were carried out for background characterisation and with an iron sample for normalisation purposes.

Data reduction of the capture measurements at GELINA is in progress and final results will be published together with the results of the experiment carried out at J-PARC facility.

3. Transmission on natural lead and ^{206}Pb

Pablo Romojaro¹, Carlos Paradela², Sonia Panizo³, Gery Alaerts², Luca Fiorito¹, S. Kopecky², Antonin Krasa¹, S. Moscati², P. Schillebeeckx², Alexey Santovskiy¹, Gert Van Den Eynde¹, Danny Vendelbo², Ruud Wynants², Vicente Bécares³, Francisco Álvarez-Velarde³,

¹Belgium Nuclear Research Center (SCK CEN), Brussels, Belgium

² European Commission, Joint Research Centre, Geel, Belgium

³Centro de Investigaciones Energéticas, Medioambientales y Tecnológicas (CIEMAT), Madrid, Spain

Lead is an important element for fast nuclear reactors and accelerator driven systems using lead or lead-bismuth eutectic as a coolant material or spallation target. Detailed sensitivity studies within the CHANDA project revealed that improved total cross section data for the main lead isotopes were required. To improve the experimental data for a new evaluation of neutron interactions with lead transmission measurements at JRC GELINA facility. A set of lead samples which include natural lead and isotopically enriched samples in ^{206}Pb and ^{208}Pb were

proposed for measurement. Transmission measurements on ^{206}Pb and natural lead samples have already been performed, while the measurement on ^{208}Pb has been postponed due to the lack of a suitable sample for transmission studies.

3.1. Experimental description

As in the bismuth case, the measurements were carried out at the 50 m transmission station of flight path 4 with the accelerator operated at 400 Hz. The conventional detection system consisting of one Li-glass scintillator connected to analogue electronics was used. Background filters were used to study the background conditions. During the ^{206}Pb measurements a bismuth permanent filter replaced the natural lead filter which is usually used in the facility to reduce the impact of the γ -flash. The experiments were carried out during 2022 and 2023. The delay was due to unattended maintenance works required at GELINA accelerator during second half of 2022. The total beam time accounted for 6 weeks including short runs with additional filters.

3.2. Data reduction and results

The data reduction has been accomplished by JRC staff and the CIEMAT PhD Sonia Panizo in the framework of the Lead_GELINA project (RIAA N° 36225/ 6 / 2021-1-RD-EUFRAT-GELINA). The transmission data analysis for the ^{206}Pb sample has been already completed and results compared to JEFF-3.3 evaluation are shown in Figure 4. The data analysis for the $^{\text{nat}}\text{Pb}$ sample is currently in progress. A technical report similar to the one published for the ^{209}Bi work will be produced to support the final data submission to the EXFOR database.

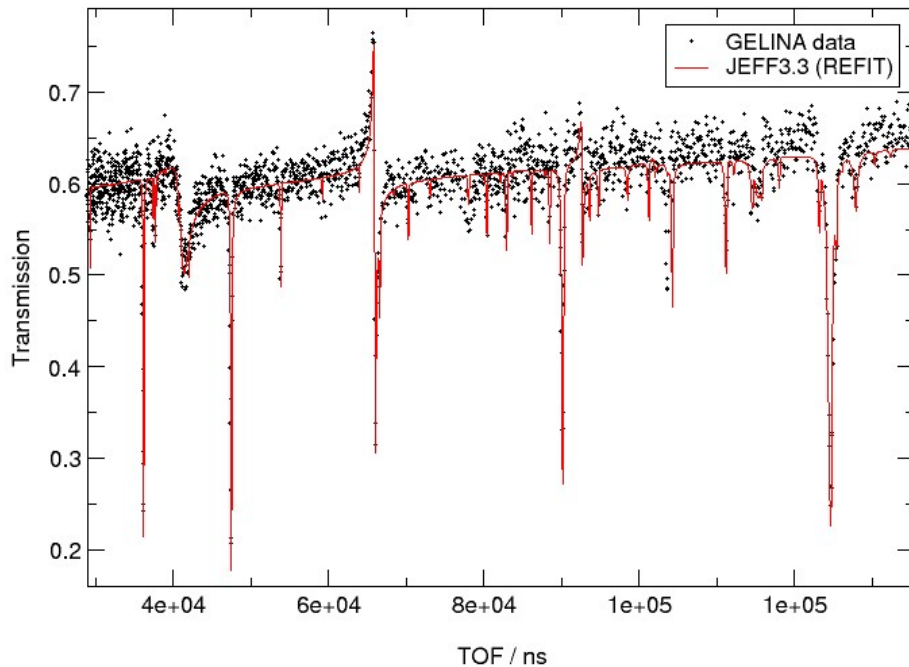


Figure 5. Comparison of the experimental and calculated transmission through the ^{206}Pb sample. The calculated transmissions are obtained with REFIT code [11] using the resonance parameters in JEFF-3.3 evaluated library.

4. $^{238}\text{U}(n,\text{inel})$ cross sections measurements at GELINA

Maëlle Kerveno¹, Catalin Borcea², Marian Boromiza², Philippe Dessagne¹, Greg Henning¹, Alexandru Negret², Markus Nyman³, Adina Olacel², Eliot Party¹, Arjan Plompen³

¹Université de Strasbourg, CNRS, IPHC/DRS UMR 7178, Strasbourg, France

²Horia Hulubei National Institute of Physics and Nuclear Engineering, Bucharest-Magurele, Romania

³European Commission, Joint Research Centre, Geel, Belgium

4.1. The prompt γ -ray spectroscopy method for (n, n') studies

Among the different experimental methods used for (n, xn) reaction studies, our collaboration has chosen the prompt γ -ray spectroscopy which, coupled to time-of-flight measurement allows the experimental determination of $(n, n'\gamma)$ cross section at the JRC-Geel GELINA facility. From the measured cross sections, the total neutron inelastic scattering and level production cross sections can be inferred as illustrated in Figure 6.

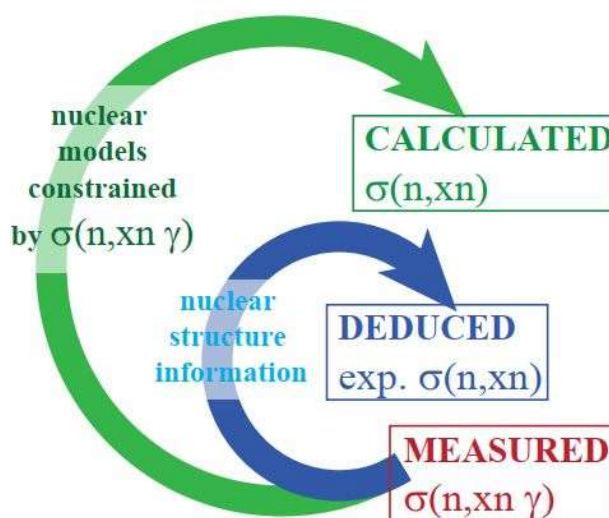


Figure 6 Schematic view of the two ways to deduce total (n, xn) cross section from measured $(n, n'\gamma)$ ones. From reference [12]

4.2. Experimental conditions

The GRAPhEME setup is installed at 30 m from the GELINA neutron source, a distance which appeared as a good compromise between neutron energy resolution and available actinides quantities for sample making. During the ^{238}U measurement campaign, it was composed of four planar HPGe detectors surrounded by a Pu-Cd-Cu shielding to protect the Germanium crystal from neutron and γ backgrounds. The HPGe crystals have typical thickness around 2-3 cm and diameter around 5-6 cm. They are placed around the sample at 110° and 150° with regards to the neutron beam to allow the precise angular integration of the γ -ray production cross sections. A fission chamber, loaded with a thin layer of ^{235}U ($^{235}\text{UF}_4$ with an areal density of $0.324(2) \text{ mg/cm}^2$), is present upstream GRAPhEME and is used for neutron flux determination. The signals (time and energy) from the detectors are recorded by a digital

acquisition system based on TNT2 cards [13] (14 bits for amplitude resolution and a 100 MHz sampling frequency). The efficiency of each HPGe detector has been precisely studied with source measurements (^{152}Eu) coupled with MCNPX [14] simulations. To take into account the spatial distribution of the neutron beam (55 mm in diameter), source measurements have been performed with point sources at different positions relative to the centre of the beam and also with an extended source. If the sample is radioactive, the radioactive decay can also be used for efficiency calibration. Once the detectors geometry is well defined, the production for each γ transition is simulated including the ^{238}U sample to take into account the self-absorption of the γ 's in the sample. For the fission chamber, as described in reference [15], its operation has been optimized to maximize the efficiency of detection.

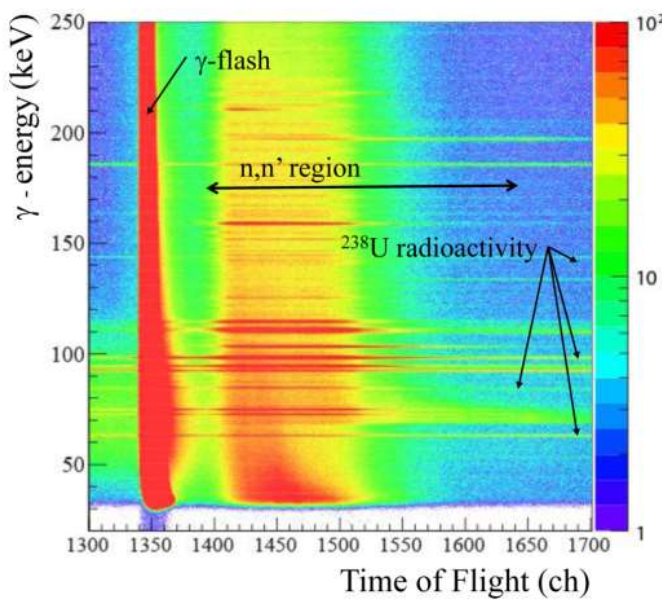


Figure 7 presents a part of the two-dimensional (γ -ray energy versus time of flight) distribution obtained for one detector during the ^{238}U measurement campaign. At a flight path of 30 m and with the time resolution of the Germanium detectors, the typical neutron energy resolution achieved is 10 keV at $E_n = 1$ MeV.

Figure 7 Two-dimensional plot for γ -ray energy (keV) as a function of the time of flight (channels) where one sees the γ rays from different sources (γ -flash, ^{238}U radioactivity, (n, xn) reactions, etc.). Figure from reference [16].

From the manufacturer, we obtained a ^{nat}U sample which is a rolled sample (disk) made of 99.9% natural uranium with a diameter and thickness of respectively 70.0(5) mm and 0.18(4) mm, according to the specifications of Goodfellow. The sample was characterized by the target laboratory of EC-JRC-Geel (Belgium). The measurements give a mass of 10.61911(7) g and diameter and thickness of 70.16(3) mm and 0.181(6) mm, respectively. The given uncertainties of the thickness and a diameter are the standard deviations of several measurements. These numbers lead to an apparent density of 15.173 g/cm^3 which does not correspond to the one of pure metallic uranium (18.95 g/cm^3). To determine the real mass of ^{238}U , we measured with GRAPHME the γ -ray energy distribution from the radioactivity of the sample. To estimate, using MCNPX simulations, the efficiency of the HPGe detectors for these

y lines we introduce oxidation to take into account the apparent density. As already done in the work mentioned in reference [15], the sample is considered to have a core of natural uranium (density 18.95 g/cm³) surrounded by layers of UO₂ (density 10.97 g/cm³); the thicknesses of the different regions are deduced using the apparent density. The determination of the ²³⁸U mass was made using the 1001.03 keV γ line from ²³⁸U radioactivity registered in the four HPGe detectors. The result is the average of nine measurements which leads to a mass of ²³⁸U equal to 10.54(23) g. More than 3000 hours of beam time have been collected during different campaigns over three years. After a strict selection of good events, the collecting time amounts to 2139 h for two HPGe detectors and 731 h and 1139 h for the two others.

4.3. Results

4.3.1. Extraction of γ -ray production cross sections

The very good energy resolution of the germanium detectors (0.7 keV at 122 keV) and time-of flight measurement allow a precise selection of γ rays from (n, n'), (n, 2n), and (n, 3n) processes and their discrimination in respect to other background γ lines (radioactivity, fission products, shielding materials). Finally, 18 γ ray transitions have been identified as γ ray in ²³⁸U and associated cross sections have been calculated. Table 1 shows the γ -transitions studied in this work.

Table 1. List of γ -transitions studied in this work. From reference [16].

TABLE II. Selection of identified γ energies [38] in the ²³⁸U energy spectra stemming from the ²³⁸U(n, n') reactions. The possible contamination of the peak in the spectra is mentioned in the three last columns. Levels are labeled as J_k^Π where J is the level total angular momentum, $\Pi = +/ -$ its parity, and k counts the levels of the same J^Π by increasing excitation energy.

E_γ (keV)	Initial state		Final state		I_γ	γ multipolarity	Peak pollution		
	E (keV)	J_k^Π	E (keV)	J_k^Π			Process	E_γ (keV)	E_{level} (keV)
44.915 (13)	44.916 (13)	2_1^+	0	0_1^+	100	$E2$	X $K\beta 3$	104.6	
103.50 (4)	148.38 (3)	4_1^+	44.916 (13)	2_1^+	100	$E2$			
							²³⁸ U(n, 2n) ²³⁷ U	103.68	159.962
159.018 (16)	307.18 (8)	6_1^+	148.38 (3)	4_1^+	100	$E2$	⁶³ Cu(n, γ) ⁶⁴ Cu	159.28	159.28
210.6 (4)	518.1 (3)	8_1^+	307.18 (8)	6_1^+	100	$E2$			
218.1 (3)	950.12 (20)	2_1^-	731.93 (3)	3_1^-	53 (6)	?	²³⁸ U(n, γ) ²³⁹ U	250.06	292.6
251.2 (7)	930.55 (9)	1_2^-	680.11 (4)	1_1^-	13.1 (14)	?			
257.8 (4)	775.9 (4)	10_1^+	518.1 (3)	8_1^+	100	$E2$			
270.1 (4)	950.12 (20)	2_1^-	680.11 (4)	1_1^-	48 (8)	?			
519.46 (8)	826.64 (11)	5_1^-	307.18 (8)	6_1^+	50 (3)	$E1$	²⁰⁸ Pb(n, n') ²⁰⁸ Pb ⁶³ Cu(n, n') ⁶³ Cu	583.19	3500
583.55 (3)	731.93 (3)	3_1^-	148.38 (3)	4_1^+	81.4 (16)	$E1$		584.82	1547
635.3 (3)	680.11 (4)	1_1^-	44.916 (13)	2_1^+	100.0 (20)	$E1$	²³⁸ U(n, 2n) ²³⁷ U	849.45 (13)	905.73 (7)
678.3 (3)	826.64 (11)	5_1^-	148.38 (3)	4_1^+	100 (6)	$E1$			
680.2 (5)	680.11 (4)	1_1^-	0	0_1^+	79 (4)	$E1$			
686.99 (3)	731.93 (3)	3_1^-	44.916 (13)	2_1^+	100 (2)	$E1$			
849.1 (4)	997.58 (7)	3_2^-	148.38 (3)	4_1^+	100 (3)	$E1$			
885.46 (10)	930.55 (9)	1_2^-	44.916 (13)	2_1^+	100 (4)	$E1$			
905.5 (5)	950.12 (20)	2_1^-	44.916 (13)	2_1^+	100 (6)	$E1$			
952.65 (7)	997.58 (7)	3_2^-	44.916 (13)	2_1^+	56.8 (13)	$E1$			

The differential cross section data for each detector (at θ_i equal to 110° or 150°) and for each neutron energy (E_n) are calculated following the formula

$$\frac{d\sigma}{d\Omega}(\theta_i, E_n) = \frac{1}{4\pi} \frac{N_{GE}(\theta_i, E_n)}{N_{FC}(E_n)} \frac{\varepsilon_{FC}\varepsilon}{\varepsilon_{GE}} \frac{\zeta_{FC}}{\zeta_{sple}} \frac{1}{\eta_{air}} \sigma_F(E_n),$$

Where N_{GE} and N_{FC} represent the dead time-corrected numbers of counts corresponding to a given γ ray in the HPGe detector i and to the fission chamber above the discrimination threshold, respectively, ε_{GE} and ε_{FC} are the germanium detector's and the fission chamber's efficiencies, σ_F is the ^{235}U fission cross section, ζ_{FC} and ζ_{sple} are the areal density (atoms/cm²) of target nuclei in the ^{235}U deposit and in the sample, and η_{air} is a correction factor which takes into account the attenuation of neutron beam between the fission chamber and the ^{238}U sample. From these differential cross section at the two angles, we can deduce thanks to the Gauss quadrature, the total γ production cross section with the formula:

$$\sigma_\gamma = 2\pi \left[\omega_1 \frac{d\sigma}{d\Omega}(\theta_1) + \omega_2 \frac{d\sigma}{d\Omega}(\theta_2) \right],$$

where $\omega_1 = 0.69571$ and $\omega_2 = 1.30429$ are the weights associated with the angles 150° and 110° respectively. It should be noticed that the cross sections correspond to γ production only and are not corrected for internal conversion.

We have paid particular attention to the estimation of systematic uncertainties (see Table 2) associated with the quantities involved in the cross section formula.

Table 2. Values and uncertainties of the parameters used in the cross section. From reference [16].

TABLE I. Values and uncertainties of the parameters used in the cross section formula, Eq. (1).

Parameter	Values	Uncertainty (%)
$N_{GE}(E_n)$	100–7000	80–1.5
$N_{FC}(E_n)$	10^4 – 10^5	$\simeq 1$
ε_{FC}	0.94	2.1
$\varepsilon_{GE}(E_\gamma)$	3×10^{-3} – 1×10^{-4}	3
ζ_{sple}	6.897×10^{20} at. cm ⁻²	2.4
ζ_{FC}	8.3×10^{17} at. cm ⁻²	0.55
$\sigma_F(E_n)$	1–2 b	1.3–1.5
η_{air}	0.98	1

Finally, it should be noticed that a special correction has been applied for the γ rays with energy below 200 keV to take into account the well-known “walk” effect of the constant fraction discriminator (CFD): the signal produced by low energy γ rays is very weak (near the level of noise) and the CFD digital algorithm can encounter difficulties when extracting the time information. That results in incorrect time assignment for events with energies below around 200 keV. To correct this effect the following procedure was applied: dedicated beam time was used with a fast-timing amplifier between the preamplifier and the TNT cards. In this way, the amplification of the output signal of the preamplifier was increased (the energy range was thus reduced) to shift the low γ -energy transitions beyond the shift induced by the CFD.

The time distributions, for the two settings and for the four detectors, are compared and the time correction is estimated. The methodology and results are illustrated in Figure 8.

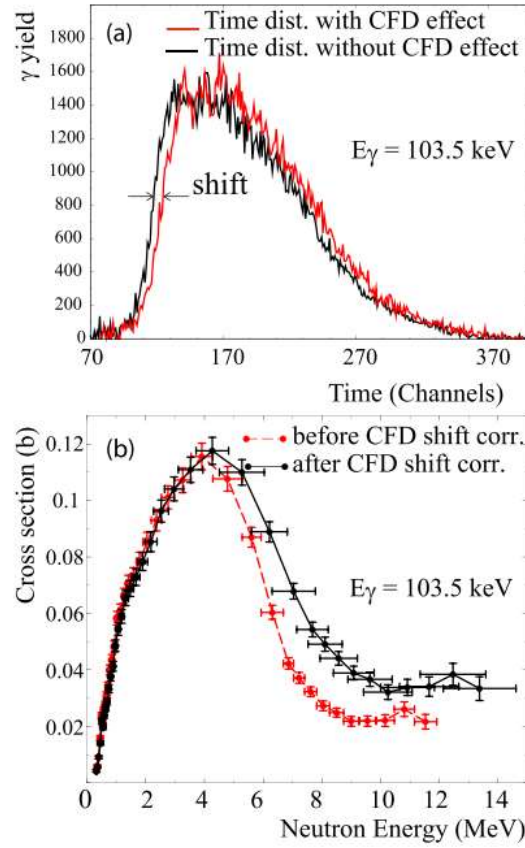


FIG. 6. (a) Time distributions for the detector G110 and for γ energy at 103.5 keV. The black distribution is not affected by CFD shift while the red one is. These two distributions are used to define the time correction to apply to the data for each impacted γ transition. (b) Cross section data for the 103.5-keV γ transition before the CFD shift correction (in red) and after (in black).

Figure 8 Illustration of the methodology for the “CFD correction” and the results on the 103.5 keV γ transition. From reference [16].

4.3.2. $(n,n' \gamma)$ cross sections

The cross sections deduced in this work are presented in Figure 9 and Figure 10. There are compared to model calculations. All details of this theoretical work can be found in reference [16].

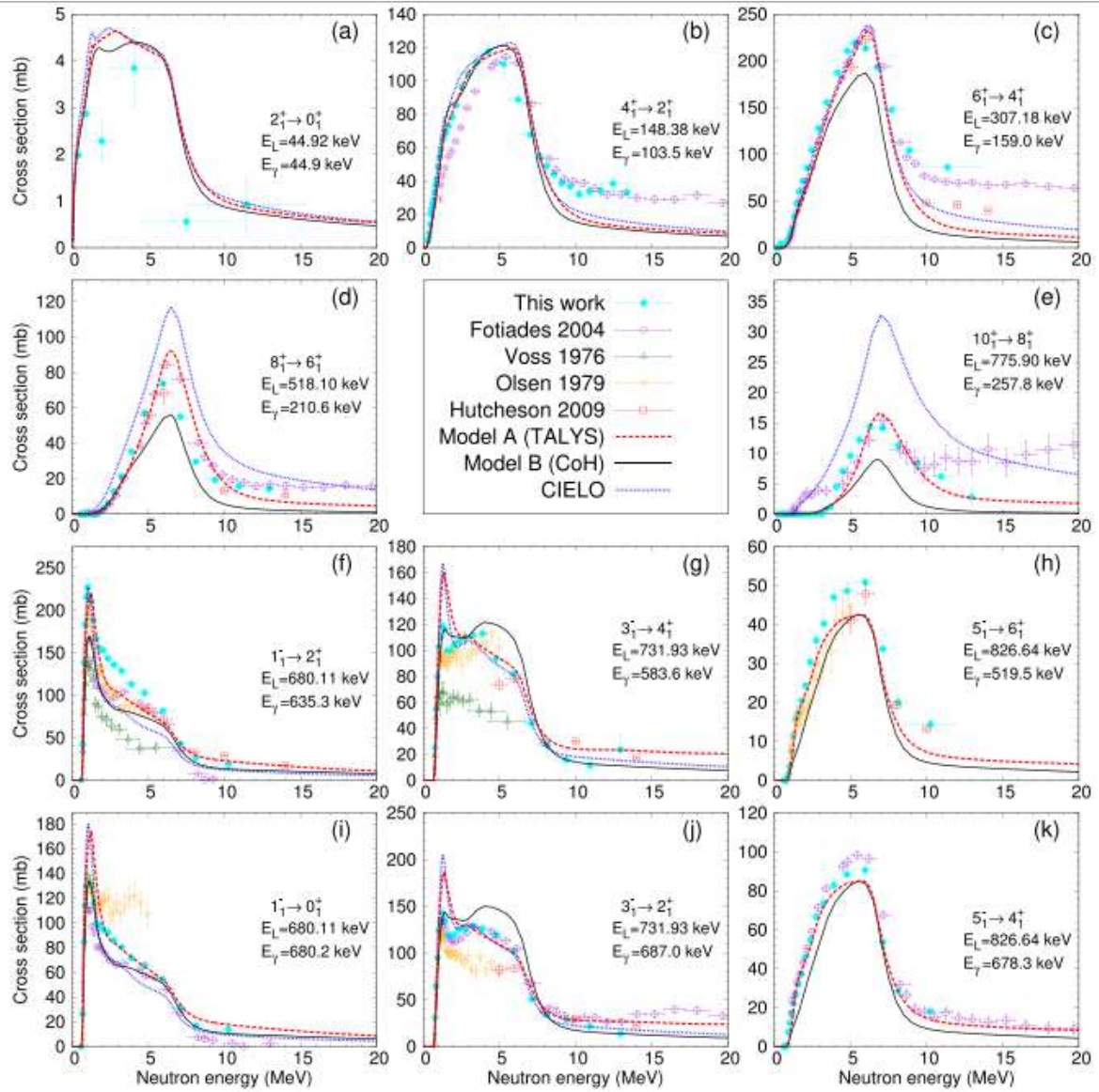


FIG. 7. Experimental $^{238}\text{U}(n, n'\gamma)$ cross sections (symbols) for E2 transitions in the GS band [panels (a)–(e)] or from the levels of the first $K^\pi = 0^-$ octupole-vibration band to the GS band [panels (f)–(k)], compared to calculations (curves; see details in Sec. IV). The Olsen datum at 680.2 keV corresponds to the sum of the 680.2-keV ($1_1^- \rightarrow 0_1^+$) and 678.3-keV ($5_1^- \rightarrow 4_1^+$) transitions.

Figure 9 Experimental $^{238}\text{U}(n, n'\gamma)$ cross sections (symbols) for E2 transitions in the GS band [panels (a)–(e)] or from the levels of the first $K = 0^-$ octupole-vibration band to the GS band [panels (f)–(k)], compared to calculations. From reference [16].

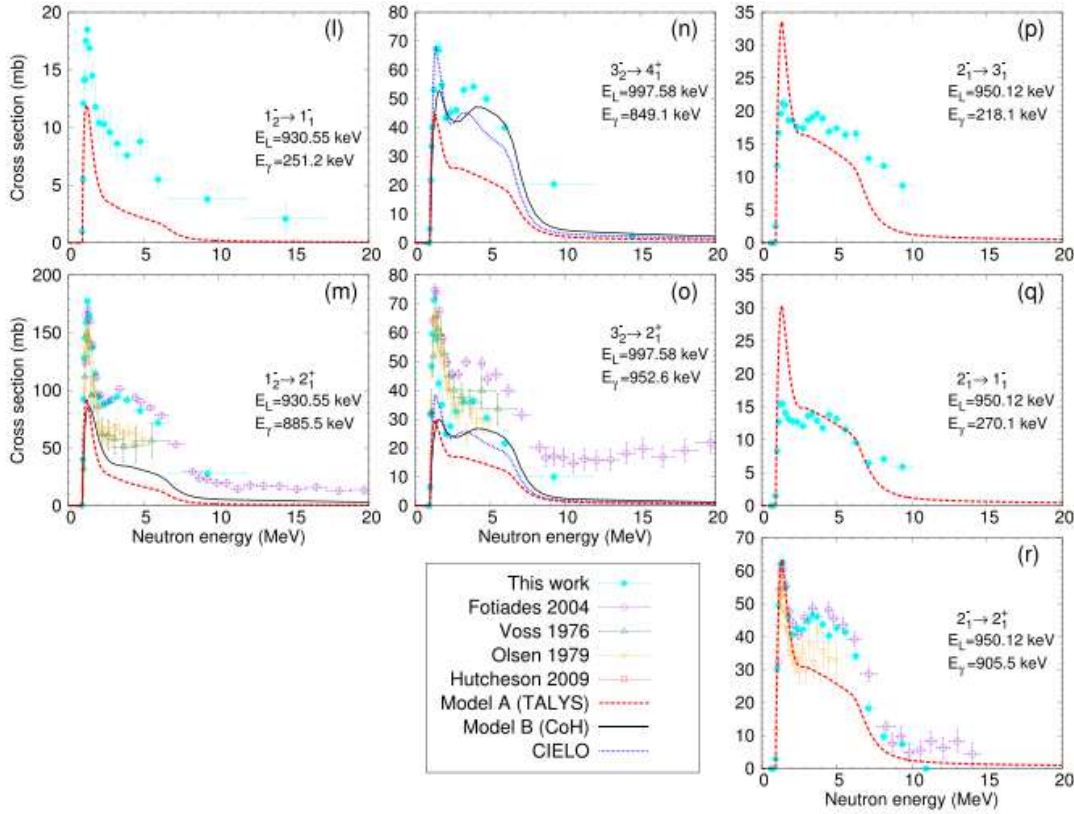


FIG. 8. Same as Fig. 7 for transitions from levels in the $K^\pi = 1^-, \alpha = 0$ band [46] [panels (p)–(r)] and in the $K^\pi = 1^-, \alpha = 1$ band [46] [panels (l)–(o)] bands.

Figure 10 Same as Fig. 9 for transitions from levels in the $K = 1-, \alpha = 0$ band [panels (p)–(r)] and in the $K = 1-, \alpha = 1$ band [panels (l)–(o)] bands. From reference [16].

4.3.3. Branching ratios

Table 3 : γ intensities calculated in this work compared to ENSDF and Govor et al. [18] values. Table from reference [16].

TABLE IV. γ intensities calculated in this work compared to ENSDF and Govor et al. [67] values.

E_{level} (keV)	E_γ (keV)	I_γ this work	I_γ ENSDF	I_γ Govor et al.
680.11	680.2	61 (7)	79 (4)	61
	635.3	100	100 (2)	100
731.93	583.55	84 (3)	81.4 (16)	85
	686.99	100	100 (2)	100
826.64	519.46	55 (2)	50 (3)	56
	678.3	100	100 (6)	100
930.55	251.2	11 (2)	13.1 (4)	8.7
	885.46	100	100 (4)	100
950.12	270.1	28 (3)	48 (8)	37
	218.1	41 (8)	53 (6)	27
997.58	905.5	100	100 (6)	100
	952.65	64 (9)	56.8 (13)	55
	849.1	100	100 (3)	100

An important ingredient in the prompt γ -ray spectroscopy method is the good knowledge of the nuclei structure information. With our measurements, when we are able to measure the deexcitation of a level by several γ rays, we can deduce the γ intensity and check the value in the ENSDF database [17] or in other nuclear structure experiments such as those by Govor et al. [18]. We have calculated γ intensity for all levels where it was possible and the results are

summarized in Table 3Table 1. This study reveals discrepancies between our and previous works for levels at 680.11, 950.12, and 997.58 keV.

4.4. Dissemination

Publications -

- *GRAPhEME: performances, achievements (@EC-JRC/GELINA) and future (@GANIL/SPIRAL2/NFS)*

M. Kerveno, et al. EPJ Web of Conferences 284, 01005 (2023)

hal-04221754v1

<https://dx.doi.org/10.1051/epjconf/202328401005>

- *Measurement of $^{238}\text{U}(n, n'\gamma)$ cross section data and their impact on reaction models*

M. Kerveno, M. Dupuis, et al. Physical Review C 104, 044605 (2021)

hal-03382914v1

<https://dx.doi.org/10.1103/PhysRevC.104.044605>

- *What can we learn from $(n, xn\ g)$ cross sections about reaction mechanism and nuclear structure ?*

M. Kerveno, M. Dupuis, et al. Eur. Phys. J Web of Conferences 239, 01023 (2020)

hal-02957494

<https://dx.doi.org/10.1051/epjconf/202023901023>

Conferences/workshops -

- ND2019: International Conference on Nuclear Data for Science and Technology 2019, 19-24 May 2019, Beijing, China
- ND2022: International Conference on Nuclear Data for Science and Technology 2022, 24-29 July 2022, Sacramento, USA, remotely with Gathertown
- WINS2023: Workshop on Elastic and Inelastic Neutron Scattering (WINS-2023), October 10th, 2023 to October 12th, 2023, Troy, US.

5. Conclusions

During the span of the SANDA project, most of the experimental work proposed in Task 2.3 has been carried out according with the original project. For the work on ^{209}Bi branching ratio, two capture measurements have been performed at GELINA and at J-PARC MLF facilities using different experimental techniques. The combined analysis, currently ongoing, should provide improved branching ratio information in the resolved resonance region. Additional

transmission measurements, carried out at GELINA, were reported in a technical document, which included recommendations to the evaluators, being the results submitted to EXFOR database.

On the production of total cross section for ^{208}Pb , transmission measurements were carried out at GELINA facility using same experimental technique than for ^{209}Bi one. However, because of the unavailability of a suitable ^{208}Pb sample, natural lead and ^{207}Pb samples were used instead. Results will be published and submitted to EXFOR.

Finally, a new precise measurement of $(n, xn\gamma)$ reaction cross sections on ^{238}U has been performed at the GELINA with the GRAPhEME (GeRmanium array for Actinides PrEcise MEasurements) setup. The prompt γ -ray spectroscopy method coupled to time-of-flight measurements is used to extract $(n, xn\gamma)$ cross section values which can be further combined to infer the total neutron inelastic scattering cross section. Cross section data for 18 γ transitions (five never measured before) are have been obtained and compared to the data in the literature. Emphasis is especially given to the uncertainty determination to produce partial cross section data as accurate as possible. Determination of branching ratios has been also investigated when possible.

References

1. P. Romojaro *et al.*, Report on sensitivity analysis of MYRRHA with list of key reactions, Deliverable 10.1 of CHANDA, 2015.
2. P. Romojaro *et al.*, Report on comparison of evaluated libraries and experimental data, Deliverable 10.2 of CHANDA, 2017.
3. L. Fiorito *et al.*, Nuclear data uncertainty analysis for the Po-210 production in MYRRHA, EPJ Nuclear Sci. Technol. 4, 48 (2018).
4. A. Plompen *et al.*, "The NEA High Priority Nuclear Data Request List for future needs", *International Conference on Nuclear Data for Science and Technology*, Nice, France, 22-27 April 2007, June 2008, EDP Sciences, pp. 765-768, doi: 10.1051/ndata:07419.
5. S. Endo, A. Kimura, S. Nakamura, O. Iwamoto, N. Iwamoto, G. Rovira, K. Terada, S. Meigo, Y. Toh, M. Segawa, M. Maeda, M. Tsuneyama, Nucl. Sci. And Tech. 59, 3 (2022).
6. B. Becker, C. Bastian, F. Emiliani, F. Gunsing, J. Heyse, K. Kauwenberghs, S. Kopecky, C. Lampoudis, C. Massimi, N. Otuka, P. Schillebeeckx and I. Sirakov, J. of Instrumentation, 7 (2012) P11002 – 19.
7. A. R. de L. Musgrove and J. A. Harvey, "Neutron resonance Spectroscopy on ^{209}Bi ", Australian Journal of Physics 31(1), 47 (1978).
8. C. Domingo-Pardo *et al.*, "New measurements of neutron capture resonances in ^{209}Bi ", Phys. Rev. C 74 (2006) 025807.
9. P. Romojaro, C. Paradela Dobarro, G. Alaerts, L. Fiorito, J. Heyse, S. Kopecky, S. Moscati, P. Schillebeeckx, A. Stankovskiy, G. Van Den Eynde, D. Vendelbo, and R. Wynants, Results of time-of-flight transmission measurements for ^{209}Bi at a 50 m station of GELINA, Publications Office of the European Union, Luxembourg, 2024, doi:10.2760/02812, JRC136373.
10. C. Paradela-Dobarro, J. Heyse, K. Kopecky, S. Moscati, L. Salamon, P. Schillebeeckx, D. Vendelbo, R. Wynants, Electronic setup for time-of-flight cross section measurements at GELINA, Publications Office of the European Union, Luxembourg, 2021, ISBN 978-92-76-43927-1, doi:10.2760/477469, JRC127003.
11. M.C. Moxon and J.B. Brisland, Technical Report AEA-INTEC-0630, AEA Technology (1991).
12. M. Kerveno *et al.* Eur. Phys. J. N 4, 23, (2018).
13. L. Arnold, R. Baumann, E. Chambit, M. Filliger, C. Fuchs, C. Kieber, D. Klein, P. Medina, C. Parisel, M. Richer *et al.*, in *14th IEEE-NPSS Real Time Conference, 2005* (IEEE, Piscataway, NJ, 2005), pp. 265–269.
14. MCNPX, online: <http://mcnpx.lanl.gov/>
15. M. Kerveno *et al.*, Phys. Rev. C 87, 024609 (2013).
16. Kerveno, M. Dupuis, *et al.* Physical Review C 104, 044605 (2021).
17. E. Browne and J. Tuli, Nucl. Data Sheets 127, 191 (2015).
18. L. Govor, A. Demidov, V. Kurkin, and I. Mikhailov, Phys. At. Nucl. 77, 131 (2014).